14) R.P. Davis : *Nat. Protoc.*, 3, p.1550(2008).
15) T.P. Zwaka : *Nat. Biotechnol.*, 21 p.319(2003).
16) A. Urbach : *Stem Cells*, 22, p.635(2004).
17) K. Watanabe : *Nat. Biotechnol.*, 25, p.681(2007).
18) R.P. Davis : *Blood*, 111, p.1876(2008).
19) B. Thyagarajan : *Stem Cells*, 26, p.119(2008).
20) A. Lombardo : *Nat. Biotechnol.*, 25, p.1298(2007).
21) S. Irion : *Nat. Biotechnol.*, 25, p.1477(2007).
22) H. Zaehres : *Stem Cells*, 23, p.299(2005).
23) W.M. 3rd Rideout : *Cell*, 109, p.17(2002).
24) D. Egli : *Nat. Rev. Mol Cell Biol.*, 9, p.505(2008).
25) D. Ben-Tosef : *Mol Cell Endocrinol.*, 282, p.153(2008).
26) E. Fragouli : *J. Assist Reprod Genet*, 24, p.201(2007).
27) K.D. Sermon : *Hum. Reprod*, 22, p.323(2007).
28) R. Eiges : *Cell Stem Cell*, 1, p568(2007).
29) Y.Verlinsky : Reprod Biomed Online, 10, p.105(2005).
30) S.J. Pickring : Reprod Biomed Online, 10, p.390(2005).
31) T. Turetsky : *Hum. Reprod.*, 23, p.46(2008).

6. フィーダーレイヤー

阿久津英憲・梅澤明弘

要旨

幹細胞を自在に扱うことが可能となることで，生命科学の基礎研究は大きく進展し，特にヒトES細胞やiPS細胞などの多能性幹細胞研究の進展による社会貢献は大きく期待されている。多能性幹細胞を樹立し，適切に培養維持するための培養環境ではフィーダーレイヤーが幹細胞の足場と培地の「conditioning」として重要な役割を果たし，安定的な増殖と未分化維持に機能する。本稿では，フィーダーレイヤーとしての概念から機能について解説し，ヒト多能性幹細胞培養に必要な性質と使用時の具体的な注意点を述べ，ヒト多能性幹細胞研究の発展に寄与したい。

キーワード

ES細胞，iPS細胞，フィーダーレイヤー，フィーダー細胞，MEF，未分化維持，STO細胞，細胞増殖，$p16^{INK4a}$，マイトマイシンC，X線照射

❖ はじめに

幹細胞を自在に扱うことが可能となることで，生命科学の基礎研究は大きく進展し，特に創薬や細胞治療など社会が身近に恩恵を受けることができる領域の研究開発が活発になってきている。特に，ヒトES細胞やiPS細胞などの多能性幹（PS）細胞研究の進展による社会貢献はたいへん期待されている。PS細胞を樹立し，適切に培養維持するための培養環境ではフィーダーレイヤーがPS細胞の足場と培地の「conditioning」として重要な役割を果たし，PS細胞の安定的な増殖と未分化維持に機能する。本稿では，フィーダーレイヤーとしての概念から機能について解説し，ヒトPS細胞培養に必要な性質と使用時の具体的な注意点を述べ，ヒトPS細胞研究の発展に寄与したい。

Ⅰ．フィーダーレイヤーのはじまり

1940年代の細胞培養系におけるチャレンジの1つには，より均一な集団としての細胞群を樹立し培養維持することにあった。しかし，たった1つの細胞からサブクローン化するために細胞を増殖させていくことは不可能であった。Earleらは細胞がクローン化できないのは，培養液中に細胞増殖のための何らかの成分が足りないためではないかという仮説のもと，よく増殖している細胞の培養液上清（「conditioned medium」概念の誕生）を使って培養したところ，単一細胞由来のクローン化に初めて成功した[1]。さらに，conditioned mediumだけでは増殖できない細胞種も多く，培養できにくい細胞が存在していたが，Puckらは細胞間相互作用の必要性もあると考え，「feeder cell」の概念を構築し，X線照射により増殖を停止させたフィーダーレイヤーと共培養するシステムが非常に有用であることを報告した[2]。1950年代には，増殖を停止させた線維芽細胞をフィーダーレイヤーとして細胞間相互作用と培地のconditioning効果を応用し，増殖しにくい細胞を増殖維持させる共培養システムが構築された。

増殖を停止させた線維芽細胞をフィーダーレイヤーとして共培養系に使用することで，増殖・培養維持が難しい細胞も効果的に培養することが可能となってきた。フィーダーレイヤーは対象となる細胞との細胞間相互作用や適切な細胞外マトリクスを提供すること[3]，そしてフィーダー細胞からの産生因子が直接または間接的に細胞間に作用し培地を細胞増殖に適切なコンディションにもっていく作用も有する（図❶）。

図❶ フィーダーレイヤーと幹細胞の相互間作用

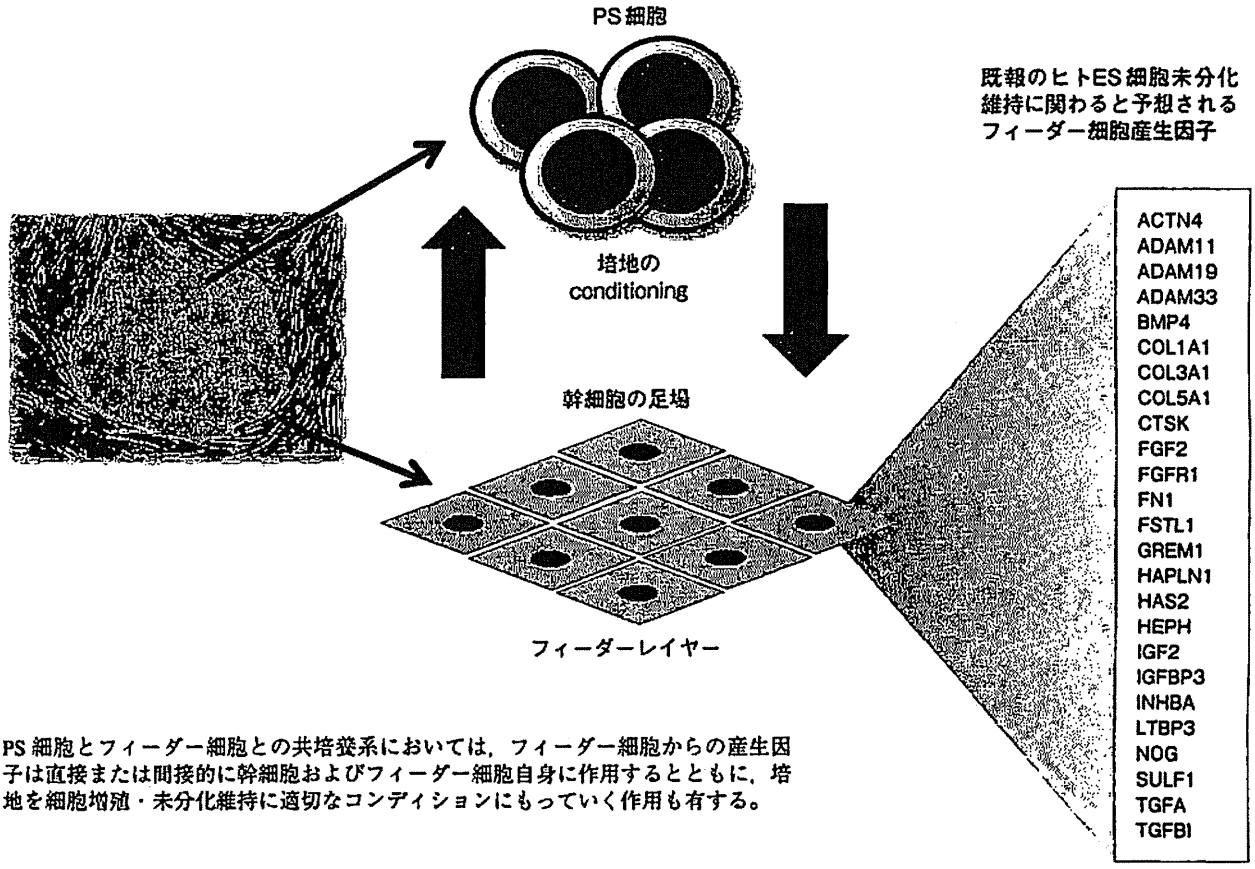

PS細胞とフィーダー細胞との共培養系においては，フィーダー細胞からの産生因子は直接または間接的に幹細胞およびフィーダー細胞自身に作用するとともに，培地を細胞増殖・未分化維持に適切なコンディションにもっていく作用も有する。

Ⅱ．フィーダーレイヤーと幹細胞

フィーダーレイヤーは多能性幹細胞であるES細胞やiPS細胞の未分化性を保持したまま維持する現在のルーチン化した幹細胞培養系[4][5]に必要であるが，ここではPS細胞に対するフィーダー細胞の機能について再確認して，ヒトPS細胞の安定的な培養維持，そして基礎および応用研究の推進に貢献できることを望む。多能性幹細胞の研究は1950年代にEC細胞が樹立され培養維持されることで本格的に始まり，後のES細胞研究へと展開していった。フィーダーレイヤーはマウスEC細胞のクローナルな増殖と未分化維持の目的で使用され，当初よりX線照射またはマイトマイシンC処理による増殖を停止させて共培養するシステムがとられた[6]。EC細胞で確立されてきたフィーダーレイヤーによる培養システムによって，胚盤胞からマウスES細胞の樹立培養が初めて報告され[7]，ヒトES細胞でも樹立と安定培養に貢献してきている[8]。PS細胞培養に対してフィーダー細胞としての機能的役割としては，①未分化性の維持，②増殖性の担保，③分化阻止，④ゲノムの安定，が求められる。Evansらによってフィーダー化したSTO細胞によってマウスEC細胞がシングル細胞レベルからクローン化でき，さらに多分化能も保持していることが示された[6]。Evansらは，同様にSTO細胞を用いて胚盤胞内部細胞塊からES細胞を樹立することでき[7]，2007年にノーベル医学・生理学賞を受賞することになる。Puckらがフィーダー細胞の概念を構築し，有用性を示したのは共培養する細胞の増殖性を示したものであり（増殖性の担保），70年代のEvansらによるEC細胞とES細胞を用いた研究によって未分化性の保持機能が示されてきた（未分化性の維持）。未分化性の保持と分化阻止機能とは同様な意味合いをもつが，共培養系に使用する細胞の種類によっては幹細胞を積極的に特定の分化系列へ分化誘導することが知られており，フィーダー細胞の機能として未分化性の保持と分化阻止機能は分けて捉えるべきと考える。分化誘導系へのフィーダーレイヤー応用例としては，Sasaiらによる PA6 間質細胞を用いた

図❷　MEF上で良好に維持されているヒトES細胞

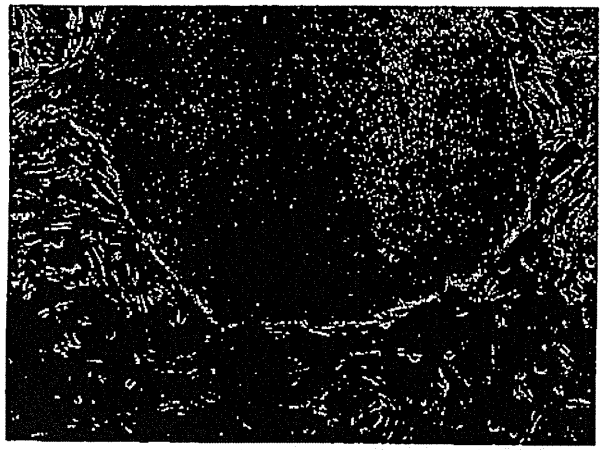

SDIA法が神経細胞分化で汎用されている[9]。SDIA法によりマウスES細胞は短期間（5日以内）に高効率（90%以上）で神経系細胞への誘導が可能である。さらに，マウスES細胞のみならずヒトES細胞に対しても，ドーパミン産生神経細胞や運動神経など疾患特異的な神経細胞へも高率に分化誘導可能である。フィーダーレイヤーの機能としてゲノムの安定性に作用することが予想される。ヒトケラチノサイトとフィーダーレイヤーとの共培養系による実験では，培養による$p16^{INK4a}$の発現を遅延させることで細胞老化（senescence）を抑制している[10]。幹細胞に関するフィーダーレイヤーとゲノムの安定性についての直接的な報告はないが，ゲノムの安定性について疑わせる例として，Thomsonらがフィーダーレイヤーなしの条件で2細胞株のヒトES細胞の樹立に成功したものの2つとも染色体異常をきたしていた[11]。

PS細胞培養でのフィーダーレイヤーの役割は，①未分化性の維持，②増殖性の担保，③分化阻止，④ゲノムの安定が担保されることであり，このすべてが満たされることが良質なフィーダー細胞の条件である。PS細胞に対して一般的に汎用されているフィーダー細胞はマウスSTO細胞とmouse embryonic fibroblast（MEF）であるが，マウスES/iPS細胞培養では，フィーダーレイヤーの質によりES/iPS細胞培養の安定性が大きく影響されることは少ない。MEF上で良好に維持されているヒトES細胞を示す（図❷）。言い換えると，マウスES/iPS細胞はフィーダーレイヤーの質に対して許容範囲が大きいことになる。しかし，ヒトPS細胞であるES/iPS細胞培養では，フィーダーレイヤーの質の低下に対して敏感であり，未分化-分化のバランスが破綻しやすい。フィーダー細胞の管理には慎重になるべきである。以下にヒトPS細胞を培養する際のフィーダー細胞調整および培養の注意点を述べる。

Ⅲ．ヒトES/iPS細胞培養時のフィーダーレイヤー調整の注意点

今回は，一般的にも汎用され筆者らの研究室でも使用しているMEFの取り扱いについて実際的な注意点を述べたい。MEF作製や使用のプロトコルに関しては成書に詳しいので参考にされたい[12][13]。ここでは，概略的に各ステップを再確認していきたい。まず，用いるマウス系統は，C57BL/6，129/sv，Balb/C，ICRなどで，12.5～13.5日目の胚から樹立される。筆者らはICRを使用しているが，純系ラインのほうが安定して質の高いMEFが獲得できるとの報告もある[12]。胚を取り出した後，四肢，頭部，腹腔内および胸腔内臓器を取り除き個体をミンチ・酵素処理するが，処理する酵素によってはフィーダー細胞内でヘテロの割合が高くなる。初代培養に使用するMEF樹立培地でのウシ胎児血清（FBS）によってもその増殖性が左右されるので，筆者らはヒトiPS細胞培養用のMEF培地作製ではFBSの製品チェックを行っている。細胞には，X線照射かマイトマイシンC処理による増殖を停止させて共培養するシステムがとられているが，われわれはX線照射処置（30Gy；1Gy/min，30min）を行っている。増殖停止の処置では，各自で選択している方法により細胞の分裂が確実に停止していることを確認することをすすめる。例えば，BrdUの取り込み解析により少なくとも90%以上の細胞が分裂停止状態であることが必要である。不十分な処置により，ヒトESやiPS細胞培養が不安定で実験の再現性に影響を与える場合がある。先にも述べたように，ヒトES細胞やiPS細胞培養はフィーダーレイヤーの質に影響されやすい。これらのヒトPS細胞培養では，通常より「何だか分化しやすい」と感じたら，そのチェック項目にフィーダーレイヤーの質も当然疑うべきであり，疑わしい場合，そのストックは躊躇せず廃棄すべきである。新たにMEFを作製あるいは購入した場合，本格的な実験に供する前にPS細胞によるフィーダー細胞のチェックは必須である。最後に，ごくまれではあるがMEF作製時にマイコプラズマ感染をする場合もあり，特定のインキュベータではなく複数のインキュベータにわたった培養ディッシュでマイコプラズマ感染が確認できる。

50年以上前にPuckらにより示されたフィーダーレ

イヤーの概念と応用方法は，ヒトPS細胞研究が盛んになっている現在においてもその根幹は何ら変わっていない。PS細胞培養での4つのフィーダーレイヤーの役割である，①未分化性の維持，②増殖性の担保，③分化阻止，④ゲノムの安定についてフィーダー細胞培養上清を用いたプロテオーム解析による未分化性維持因子の研究[14][15]やMEFを用いた細胞増殖性担保のメカニズム解析[16]など分子レベルで幹細胞培養システムにおけるネットワークが解明されようとしている。ヒトPS細胞研究は，その臨床あるいは創薬などの生命医科学応用へと進展している。MEFと培地にウシ胎児血清代替物を用いる現在の標準化した培養方法下でのヒトES細胞では，通常ヒトには存在しない異質な糖鎖（Nグリコリルノイラミン酸）の発現が認められ，免疫原性にもなりうることから，幹細胞応用の先を見据えた場合，Xeno-Free systemによる培養の実現が必要になる。ヒト組織由来のフィーダー細胞やフィーダー細胞を使用しない培養システム開発がどんどん進んでいる。フィーダー細胞から捉えるヒト幹細胞研究のアプローチはいまだ重要なストラテジーであると考えられる。

参考文献

1) Sanford KK, Earle WR, et al : J Natl Cancer Inst 9, 229-246, 1948.
2) Puck TT, Marcus PI : Proc Natl Acad Sci USA 41, 432, 1955.
3) Ehmann UK, Stevenson MA : Exp Cell Res 243, 76-86, 1998.
4) Akutsu H, Cowan CA, et al : Methods Enzymol 418, 78-92, 2006.
5) Park IH, Lerou PH, et al : Nat Protoc 3, 1180-1186, 2008.
6) Martin GR, Evans MJ : Proc Natl Acad Sci USA 72, 1441-1445, 1975.
7) Evans MJ, Kaufman MH : Nature 292, 154-156, 1981.
8) Thomson JA, Itskovitz-Eldor J, et al : Science 282, 1145-1147, 1998.
9) Kawasaki H, Mizuseki K, et al : Neuron 28, 31-40, 2000.
10) Ramirez RD, Morales CP, et al : Genes Dev 15, 398-403, 2001.
11) Ludwig TE, Levenstein ME, et al : Nat Biotechnol 24, 185-187, 2006.
12) Crook JM, Horne R, et al : The Practical Handbook (Sullivan S, Cowan C, et al eds), John 53-80, JohnWiley & Sons, 2007.
13) Stubban C, Wesselschmidt RL : Human Stem Cell Manual (Loring JF, Wesselschmidt RL, et al eds), 34-46, Elsevier, 2000.
14) Lim JW, Bodnar A : Proteomics 2, 1187-1203, 2002.
15) Prowse AB, McQuade LR, et al : J Proteome Res 6, 3796-3807, 2007.
16) Artero-Castro A, Callejas FB, et al : Mol Cell Biol 29, 1855-1868, 2009.

阿久津英憲

プロフィール

1995年　弘前大学医学部卒業
福島医科大学産婦人科入局
1999年　ハワイ大学幹細胞研究室留学
2005年　国立成育医療センター研究所生殖・細胞医療研究部生殖技術研究室長

現在は，ヒトES細胞樹立研究を中心に行っている。

米国における細胞治療システムの課題

Challenges for the appropriate model of stem cell therapy in the United States

Mahendra Rao
Vice President, R & D of Primary Stem Cell systems, Life technologies

(訳)三浦　巧・阿久津英憲(国立成育医療センター研究所生殖・細胞医療研究部)

細胞治療を主にした再生医療の確実な成功には，①成人，胎児および胚性の組織から大量の“正常な”細胞が獲得できることと，②臨床的な症状の改善または治癒を維持するための十分な期間，移植した細胞が生体内で増殖し，維持され，適切な機能を果たすことが約束されなければならない．一般的に，自家組織から移植に必要な大量の細胞を獲得することは困難であるため，たとえば複数の培養ケースから細胞を得，最終的に集めて必要な細胞数を得たり，増殖能が高い前駆細胞やES細胞などの幹細胞を用いて特定の細胞へ分化誘導させ十分な量の細胞を獲得する必要がある．最近では，増殖能がない分化した細胞を使う方法が編み出されてきた．分化細胞に転写因子や調節因子などの外来遺伝子を導入したり低分子化合物を添加することにより，分化多能性を獲得させES細胞類似の性質をもつ人工多能性幹(iPS)細胞を得ることが報告された．再生医療へのアプローチとして，自家体細胞からiPS細胞を樹立し，特定の細胞種へ分化誘導させることにより，自己由来の種々の細胞を獲得することが可能となっている．

十分な治療効果と安全性を担保した細胞治療にとって重要な課題は，治療に足る十分な細胞数を得ることであり，その細胞培養工程では品質管理と追跡可能性が確保され，各種の汚染を防いで良質な細胞を提供しなければならない．

生物製剤の製造に関するガイドラインはCMC(Chemistry, Manufacturing, and Controls)やGMP(Good Manufacturing Practice)ガイドラインに基づいて作成され，体系化されてきている．抗体医薬，遺伝子治療，ペプチド医薬や成長因子製剤などに基づく治療に関しては，CMCやGMPの基準に従って承認され，治療が遂行されているのに，細胞治療，とくに幹細胞の臨床応用に際してはさらに追加して審議する事項が存在する．

生物製剤製造プロトコールでは，基本的に未分化幹細胞のマスター細胞バンクが存在することになっていて，そのバンク化する幹細胞は規格化された明確な基準に則って，目的の機能をもつ十分量の細胞を創出することが示されていなければならない．幹細胞に関しては，とくに考慮しなければならない性質上の問題がある．つまり，培養で未分化状態を維持することはきわめて不安定であり，増殖過程で分化しやすい傾向にあるということである．その培養上の不安定性がために，実際の細胞製剤工程では，培養細胞の質を適当量の細胞を用い，迅速にその品質を評価する品質管理施策を策定することも重要であると考えられる．培養工程を複雑化していけば，最終の目的細胞の品質チェックだけでなく培養工程過程の各細胞サンプルの品質チェックの回数が増えより煩雑になると思われる．したがって，極力培養工程を簡素化できる，組織から直接培養増殖可能な細胞は品質チェックとしてのゲノム解析などは必要性がないかもしれないが，一方で，iPS細胞のように遺伝子操作が加えられた細胞は多くの品質検査(細胞機能性評価，遺伝子発現プロファイリング，ゲノム

安定性評価，エピジェネティック解析など)を受ける必要がある．そのなかでもヒストン蛋白質の修飾解析とDNAメチル化解析は，エピジェネティックの変化を解析するうえでもっとも汎用化されていると思われる．この両解析系とも労力とコストの面からも簡単にできるものではないが，最近では網羅的に行えるアレイ解析が開発され，より安価にメチル化解析が行えるようになってきている．

また，細胞製剤として応用する細胞集団から不適切な細胞を完全に除去する方法を確立することも重要である．多能性幹細胞を使用する場合，未分化細胞のままでは治療に適さないことがあることは明白であり，分化誘導した細胞を細胞ツールとして用いる方が適切であることが多い．現段階において望まれる細胞集団は，未分化細胞や他の不必要な分化細胞が除去されている状態である．現時点での分化細胞を獲得する技術応用はある程度限られたものであり，適切な細胞集団を抽出していくにはポジティブセレクションによる方法をもっと改良していかなければならず，この方法に用いる選択因子はその品質と性質を詳細に検討しなければならない．

出発物質(未分化細胞)から最終物質(分化細胞)が決まり，その生産方法(分化誘導法)がいったん確立したとしても，合理的な費用で再現よく大量の最終産物を得られなければ，その実用化は困難となるであろう．たしかに，以上の点は有効な治療法を開発していくことについて重要な開発要素であり，加えて，GMP基準を満たす必要もある．当初，GMP基準は一部の薬品製造開発のために定められ，その後，抗体医薬や蛋白質医薬のような生物製剤の製造に対する基準も盛り込まれた．現在では，細胞医薬を網羅するようにGMP基準が修正されてきている．大量生産のために課せられる厳密さや規則は一部の主要な製造モデルに基づいて定められている．しかし，モデルとなる一部の細胞に対して基準を定めることは困難であるため，GMPにおける細胞医薬に対する基準を個々の治療に対して大幅に改定する必要がある．細胞療法のようなオーダーメード医療にとって厳密な規制を設定することは重要であり，現在，監督機関はこれらの課題に取り組みはじめている．

治療にかかわる製品開発を簡略化するためにも，適切な製造工程を確立する必要がある．種々の検定基準において比較的明確化されている医薬品検定における動物実験のように，臨床試験もその評価法と判定基準は十分に確立しているが，このような低分子化合物に対する医薬品製剤としての大規模検定・評価系が細胞治療の検定・評価モデルとして適切であるか，そして追跡調査をどのくらいの期間行えばよいかなど，さまざまなオプションとともに十分に検討しなければならない．

細胞治療におけるあらたな開発要素としては，われわれはこれまでの製造工程，動物実験や臨床治験プロトコールを再評価し，今後は用いる細胞の特徴的な性質を理解したうえで，移植後の体内での長期的な細胞動態や機能そして腫瘍化等の移植前・後の性質を十分に考慮した検定・評価系を構築していくべきである．

今後，オーダーメード医療を発展させるためには，細胞治療モデルの抜本的な再評価が必要であろうし，監督機関は患者に対して安全性を担保するためのさまざまな評価方法を検討することになるであろう．

訳者付記：ラオ博士は神経細胞生物学の世界的な研究者であるとともに，ライフテクノロジーズ社の再生医療部門のバイスプレジデントであり，アメリカ内のみならず世界中の幹細胞研究の動向に熟知し，先導役も担っている．幹細胞，とくにヒトES細胞の再生医療応用に向けて，世界でももっとも早く研究を展開させてきた研究者のひとりであるとともに，国際幹細胞研究学会(ISSCR)による幹細胞治療国際ガイドラインの品質管理・製造部門委員長やFDAのBRMACなどの委員長も務めている．安心で安全に基礎研究の裏づけのある幹細胞治療の“実験台からベッドサイド”の実現のため，基礎研究，法制度そして産業化の各分野に精通したバランス感覚の優れた研究者でアメリカの幹細胞治療展開の中心にいる(阿久津英憲)．

EXPERIMENTAL CELL RESEARCH 315 (2009) 2727–2740

available at www.sciencedirect.com

ScienceDirect

www.elsevier.com/locate/yexcr

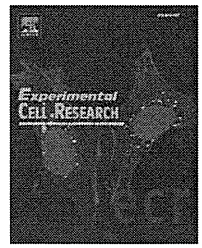

Research Article

Mesenchymal to embryonic incomplete transition of human cells by chimeric OCT4/3 (POU5F1) with physiological co-activator EWS

Hatsune Makino[a], *Masashi Toyoda*[a], *Kenji Matsumoto*[b], *Hirohisa Saito*[b], *Koichiro Nishino*[a], *Yoshihiro Fukawatase*[a], *Masakazu Machida*[a], *Hidenori Akutsu*[a], *Taro Uyama*[a], *Yoshitaka Miyagawa*[c], *Hajime Okita*[c], *Nobutaka Kiyokawa*[c], *Takashi Fujino*[d,f], *Yuichi Ishikawa*[e], *Takuro Nakamura*[d], *Akihiro Umezawa*[a,*]

[a] *Department of Reproductive Biology, National Institute for Child Health and Development, Tokyo, 157-8535, Japan*
[b] *Department of Allergy and Immunology, National Institute for Child Health and Development, Tokyo, 157-8535, Japan*
[c] *Department of Developmental Biology and Pathology, National Institute for Child Health and Development, Tokyo, 157-8535, Japan*
[d] *Department of Carcinogenesis, The Cancer Institute, Japanese Foundation for Cancer Research, Tokyo, 140-8455, Japan*
[e] *Department of Pathology, The Cancer Institute, Japanese Foundation for Cancer Research, Tokyo, 140-8455, Japan*
[f] *Department of Pathology, Faculty of Medicine, Kyorin University, Tokyo, 181-8611, Japan*

ARTICLE INFORMATION

Article Chronology:
Received 7 November 2008
Revised version received 15 June 2009
Accepted 16 June 2009
Available online 24 June 2009

Keywords:
Dedifferentiation
Mesoderm
Embryonic carcinoma
iPS cell
OCT4/3
Stem cell

ABSTRACT

POU5F1 (more commonly known as OCT4/3) is one of the stem cell markers, and affects direction of differentiation in embryonic stem cells. To investigate whether cells of mesenchymal origin acquire embryonic phenotypes, we generated human cells of mesodermal origin with overexpression of the chimeric *OCT4/3* gene with physiological co-activator EWS (product of the *EWSR1* gene), which is driven by the potent *EWS* promoter by translocation. The cells expressed embryonic stem cell genes such as *NANOG*, lost mesenchymal phenotypes, and exhibited embryonal stem cell-like alveolar structures when implanted into the subcutaneous tissue of immunodeficient mice. Hierarchical analysis by microchip analysis and cell surface analysis revealed that the cells are subcategorized into the group of human embryonic stem cells and embryonal carcinoma cells. These results imply that cells of mesenchymal origin can be traced back to cells of embryonic phenotype by the *OCT4/3* gene in collaboration with the potent cis-regulatory element and the fused co-activator. The cells generated in this study with overexpression of chimeric OCT4/3 provide us with insight into cell plasticity involving OCT4/3 that is essential for embryonic cell maintenance, and the complexity required for changing cellular identity.

Introduction

Somatic stem cells have been shown to have a more flexible potential, but the conversion of mesenchymal cells to embryonic stem (ES) cells has still been a challenge and requires gene transduction [1–4]. This phenotypic conversion requires the molecular reprogramming of mesenchyme. Mesenchymal stem cells or mesenchymal progenitors have been isolated from adult bone marrow [5], adipose tissue [6], dermis [7], endometrium [8], menstrual blood [8], cord blood [9,10], and other connective tissues [11]. These cells are

* *Corresponding author.* Fax: +81 3 5494 7048.
E-mail address: umezawa@1985.jukuin.keio.ac.jp (A. Umezawa).

0014-4827/$ – see front matter © 2009 Elsevier Inc. All rights reserved.
doi:10.1016/j.yexcr.2009.06.016

capable of differentiating into osteoblasts [12], chondrocytes [13], skeletal myocytes, adipocytes, cardiomyocytes [14,15], and neural cells [16]. However, most of the differentiation capability is limited to cells of mesodermal origin. This is in contrast to ES cells derived from the inner cell mass of the blastocyst that differentiate into cells of three germ cell layers. ES cells are pluripotent and immortal, and, therefore, ES cells provide an unlimited number of specialized cells.

Embryonic and adult fibroblasts have been induced to become pluripotent stem cells (iPS cells) or ES-like cells by defined factors including POU5F1 (also known as OCT4/3) [1–3]. OCT4/3 protein, a member of the POU family of transcription factors, is related to the pluripotent capacity of ES cells, and is thus a distinctive marker to identify primordial germ and embryonic stem cells [17–21]. OCT4/3 is down-regulated during oogenesis and spermatogenesis [22]. Furthermore, knocking out the *OCT4/3* gene in mice causes early lethality because of lack of inner cell mass formation [23], and OCT4/3 is critical for self-renewal of ES cells [24]. During human development, expression of OCT4/3 is found at least until the blastocyst stage [25] in which it is involved in gene expression regulation. OCT4/3 functions as a master switch in differentiation by regulating cells that have, or can develop, pluripotent potential by activating transcription via octamer motifs [26].

The EWS gene was originally identified at the chromosomal translocation, and fused with the ets transcription factors in Ewing sarcoma, as is the case of other sarcomas [27–30].

We report here the generation of human cells that overexpress the *OCT4/3* gene with physiological co-activator EWS (translation product of the *EWS* gene). In this study we show that the cells of mesenchymal origin overexpressing OCT4/3 can be traced back to cells with an embryonic phenotype.

Materials and methods

Cell culture

GBS6 cells were generated from primary or first passage cells of a pelvic tumor [31], and cultured in tissue culture dishes (100 mm, Becton Dickinson) in the G031101 medium (Med Shirotori, Tokyo). All cultures were maintained at 37 °C in a humidified atmosphere containing 95% air and 5% CO_2. When the cultures reached subconfluence, the cells were harvested with Trypsin–EDTA Solution (cat# 23315, IBL) at 0.06% trypsin, and replated at a density of 5×10^5 in a 100 mm dish. Medium changes were carried out twice weekly thereafter. Both H4-1 and Yub10F were human bone marrow cells. The 3F0664 were human bone marrow-derived mesenchymal cells and were purchased from Lonza (PT-2501, Basel, Switzerland). The H4-1, Yub10F and 3F0664 cells were cultured in the mesenchymal-stem-cell-growth (MSCG)-Medium-BulletKit (PT-3001, Lonza). The NCR-G1 (a human yolk sac tumor line), NCR-G2 (a human embryonal carcinoma cell line from a testicular tumor), NCR-G3 (a human embryonal carcinoma cell line from a testicular tumor) and NCR-G4 (a human embryonal carcinoma cell line) were cultured in the G031101 medium as previously described [32]. In an experiment to inhibit cell adhesion, GBS6 and NCR-G3 cells were treated with anti-human E-cadherin, monoclonal (Clone HECD-1) (M106, TAKARA BIO INC.) at 100 μg/mL. Treatment with the demethylating agent, 5′-aza-2′-deoxycytidine (5azaC; A2385, SIGMA), was performed on GBS6 cells. GBS6 cells were treated with 3 μM of 5azaC for 24 h, and then cultured without treatment for 24 h. The 5azaC-traeated GBS6 cells were described as "GBS6-5azaC". MRC-5 human fetal lung fibroblasts were maintained in POWEREDBY10 medium (MED SHIROTORI CO., Ltd, Tokyo, Japan). We used these cells at between 17 and 25 PDs for the infection of the retroviral vectors. 293FT cells were maintained in DMEM containing 10% FBS, 1% penicillin and streptomycin. iPS cells were maintained in iPSellon medium (007001, Cardio) supplemented with 10 ng/mL recombinant human basic fibroblast growth factor (bFGF, WAKO, Japan). For passaging, iPS cells were washed once with PBS and then incubated with Dulbecco's Phosphate-Buffered Saline (14190-144, Invitrogen) containing 1 mg/mL Collagenase IV (17104-019, Invitrogen), 1 mM $CaCl_2$, 20% Knockout Serum Replacement (KSR) (10828-028, Invitrogen), and 0.05% Trypsin–EDTA Solution (23315, IBL) at 37 °C. When colonies at the edge of the dish started dissociating from the bottom, DMEM/F12/collangenase was removed. Cells were scraped and collected into 15 mL conical tubes. An appropriate volume of the medium was added, and the contents were transferred to a new dish on irradiated MEF feeder cells. The split ratio was routinely 1:3.

G-banding karyotypic analysis and spectral karyotyping (SKY) analysis

Metaphase spreads were prepared from cells treated with Colcemid (Karyo Max, Gibco Co. BRL, 100 ng/mL for 6 h). We performed a standard G-banding karyotypic analysis on at least 50 metaphase spreads for each population. SKY analysis was performed on metaphase-transduced cells according to the kit manufacturer's instruction (ASI, Carlsbad, CA) and a previously published method [33].

RT-PCR

The cDNAs were synthesized with an aliquot (5 μg) of each total RNA using Oligo-(dT)20 primer (18418-020, Invitrogen) and SuperScript III Reverse Transcriptase (18080-044, Invitrogen). Both the RNA strand of an RNA–DNA hybrid and single-stranded DNA were degraded by RNaseH (18021-071, Invitrogen). For the thermal cycle reactions, cDNA was amplified by T3 Thermocycler (Biometra, Goettingen, Germany) under the following reaction conditions: 30 cycles of a PCR (94 °C for 30 s, 55 °C for 30 s and 72 °C for 30 s) after an initial denaturation (94 °C for 1 min). Primer sets used for PCR reactions are described in Tables 1 and 2. As the same amount of cDNA template was used in all reactions, in comparison to the glyceraldehyde-3-phosphate dehydrogenase (GAPDH) standard, the expression levels were evaluated. The controls consisted of reactions without reverse transcriptase in the process of cDNA synthesis.

Table 1 – PCR primers to detect the chimeric *EWS-OCT4/3* gene and untranslocated *OCT4/3* gene.

Symbol	Name	Sequence
A	EWS exon6-F	5′ TTA GAC CGC AGG ATG GAA AC 3′
B	EWS ex6 intron-F	5′ GTG GGG TTC ACT AT 3′
C	POU5F1-1a-F	5′ GAT CCT CGG ACC TGG CTA AG 3′
D	POU5F1-2-F	5′ CTT GCT GCA GAA GTG GGT GGA GGA A 3′
E	POU5F1-1a-R	5′ TCA GGC TGA GAG GTC TCC AA 3′
F	POU5F1-3-R	5′ CTG CAG TGT GGG TTT CGG GCA 3′

Table 2 – PCR primers for detection of gene transcripts.

Name	Sequence	Size (bp)
Nanog	Forward: 5′ AGT CCC AAA GGC AAA CAA CCC ACT TC 3′ Reverse: 5′ ATC TGC TGG AGG CTG AGG TAT TTC TGT CTC 3′	164
Sox2	Forward: 5′ ACC GGC GGC AAC CAG AAG AAC AG 3′ Reverse: 5′ GCG CCG CGG CCG GTA TTT AT 3′	253
UTF1	Forward: 5′ ACC AGC TGC TGA CCT TGA AC 3′ Reverse: 5′ TTG AAC GTA CCC AAG AAC GA 3′	230
GAPDH	Forward: 5′ GCT CAG ACA CCA TGG GGA AGG T 3′ Reverse: 5′ GTG GTG CAG GAG GCA TTG CTG A 3′	474

Immunoblot analysis

Whole lysates of GBS6 or NCR-G3 cells were loaded on 10% SDS/PAGE (40 μg total protein/lane) and transferred to a nitrocellulose membrane. The blots were probed with antibodies against anti-Oct3/4 (C-20 for the C-terminus of OCT4/3 of human origin; sc-8629, Santa Cruz), developed with polyclonal rabbit anti-goat Immunoglobulins/HRP antibody (P0160; Dako), and detected by chemiluminescence following the manufacturer's protocol (ECL Western Blotting Analysis System, Amersham).

Flow cytometric analysis

Cells were stained for 30 min at 4 °C with primary antibodies and immunofluorescent secondary antibodies. The cells were then analyzed on a Cytomics FC 500 (Beckman Coulter, Inc., Fullerton, CA, USA) and the data were analyzed with the FC500 CXP Software ver.2.0 (Beckman Coulter, Inc., Fullerton, CA, USA). Antibodies against human CD9 (555372, PharMingen), CD13 (IM0778, Beckman), CD14 (6603511, Beckman), CD24 (555426, PharMingen), CD29 (6604105, PharMingen), CD31 (IM1431, Beckman), CD34 (IM1250, Beckman), CD44 (IM1219, Beckman), CD45 (556828, PharMingen), CD50 (IM1601, Beckman), CD55 (IM2725, Beckman), CD59 (IMK3457, Beckman), CD73 (550257, PharMingen), CD81 (555676, PharMingen), CD90 (IM1839, Beckman), CD105 (A07414, Beckman), CD106 (IM1244, Beckman), CD117 (IM1360, Beckman), CD130 (555756, PharMingen), CD133 (130-080-801, Miltenyi Biotec), CD135 (IM2234, Beckman), CD140a (556002, PharMingen), CD140b (558821, PharMingen), CD157 (D036-3, IBL), CD166 (559263, PharMingen), CD243 (IM2370, Beckman), ABCG2 (K0027-3, IBL),

Table 3 – Expression of human ES cell-associated genes.

A

Cell		OCT4/3	SOX2	NANOG	UTF1	TDGF1	ZIC3	DPPA4	MYC	KLF4
GBS6	Flags	P	A	A	A	A	A	A	P	A
	Raw	2493	56	9	15	23	19	9	3261	171
GBS6-5azaC	Flags	P	A	A	A	A	A	A	P	A
	Raw	6620	146	19	28	20	15	11	1359	102
NCR-G1	Flags	A	A	A	A	P	P	A	A	A
	Raw	46	67	11	19	5180	2349	97	157	91
NCR-G2	Flags	P	A	P	A	P	P	P	A	A
	Raw	2093	120	3972	166	2154	389	873	160	84
NCR-G3	Flags	P	P	P	P	P	P	P	P	P
	Raw	14338	1239	14925	9208	11207	5294	4036	1086	1151
NCR-G4	Flags	P	P	P	P	P	P	P	P	A
	Raw	10602	352	9469	1684	9830	2741	2138	746	151
H4-1	Flags	A	A	A	A	A	A	A	P	P
	Raw	83	13	11	17	40	7	2	1635	489
3F0664	Flags	A	A	A	A	A	A	A	P	P
	Raw	56	63	14	34	21	21	22	735	832
Yub10F	Flags	A	A	A	A	A	A	A	P	A
	Raw	19	49	9	63	12	12	4	680	9

B

Gene symbol	Probe set ID	Gene name
POU5F1	208286_x_at	Oct4/3
SOX2	213721_at	Sox2
NANOG	220184_at	Nanog; Nanog homeobox
UTF1	208275_x_at	Utf1; undifferentiated embryonic cell transcription factor 1
TDGF1	206286_s_at	Tdgf1; teratocarcinoma-derived growth factor 1
ZIC3	207197_at	Zic3; odd-paired homolog
DPPA4	219651_at	Dppa4; developmental pluripotency associated 4
MYC	202431_s_at	c-myc
KLF4	220266_s_at	Klf4; Kruppel-like factor 4

A. Gene expression was examined with the Human Genome U133A Probe array (Affymetrix). Raw data values (*Raw*) for each gene expression are shown. *Flags*: Gene expression was judged to be "*P* (present)" or "*A* (absent)" in each cell by the GeneChip Analysis Suite 5.0 computer program. GBS6-5azaC: GBS6 cells were exposed to 3 μM 5′-aza-2′-deoxycytidine for 24 h, and then cultured without any treatment for 24 h.
B. Gene names for each symbol.

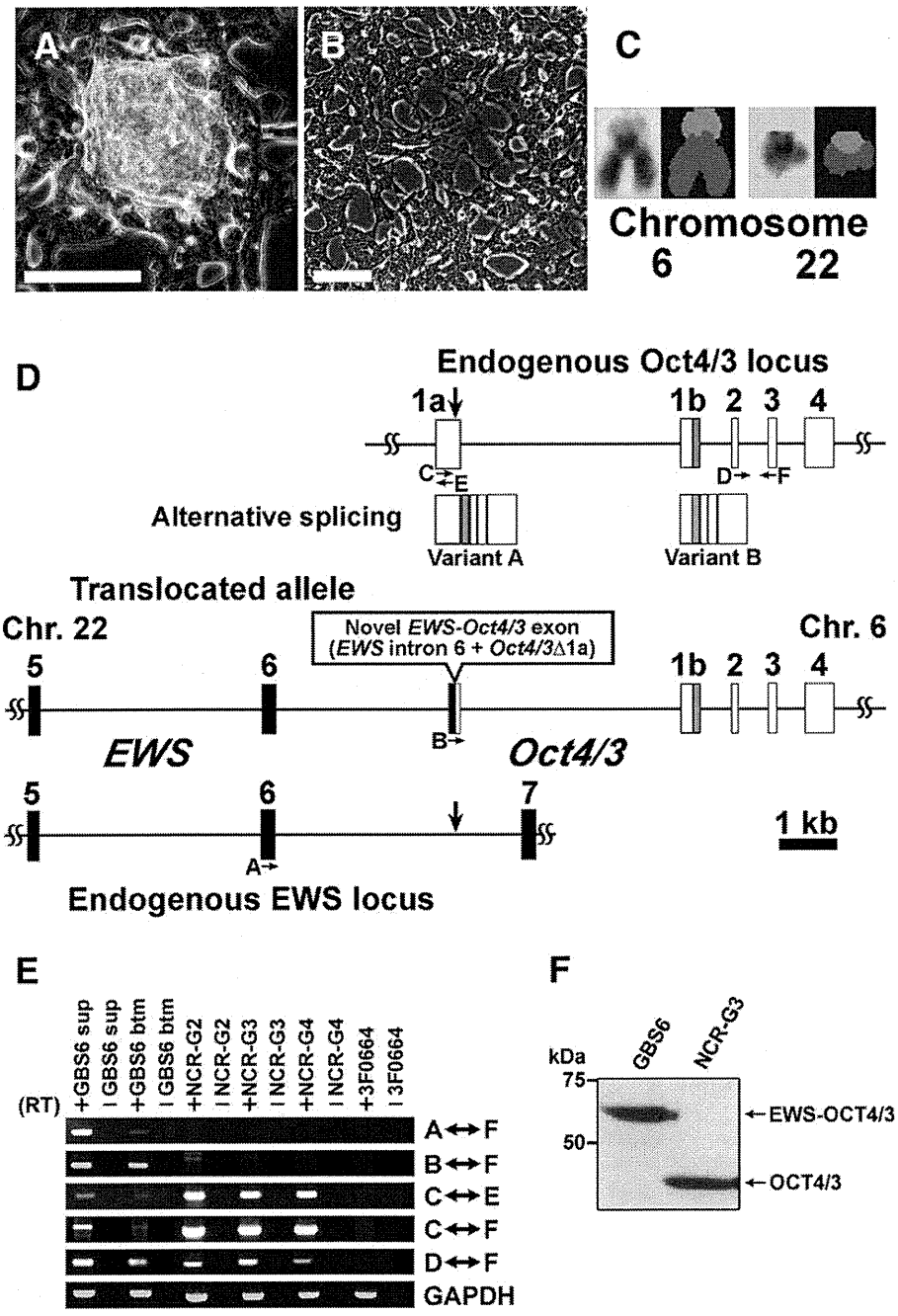

Fig. 1 – Phase contrast micrograph of GBS6 cells, and expression of the translocated *POU5F1/OCT4/3* gene. A cell line termed "GBS6" was generated from primary or first passage cells of a pelvic tumor [31]. (A) GBS6 cell aggregate (GBS6 sup). Scale bar: 100 μm. (B) GBS6 adherent cells (GBS6 btm). Scale bar: 100 μm. (C) G-banding karyotypic analysis and Spectral karyotyping (SKY) analysis of the translocated chromosomes. (D) Schematic representation of the *EWS-OCT4/3* structure in the t(6;22) tumor. *EWS* exons are represented by black boxes and *OCT4/3* exons by open boxes. The *OCT4/3*-1b exon is composed of an open and gray box. The novel *EWS-OCT4/3* chimeric exon is created by the fusion between *EWS* intron 6 and part of the exon of *OCT4/3* (Δ1a). The vertical arrows indicate each breakpoint on either chromosome 22 (*EWS*) or chromosome 6 (*OCT4/3*). The horizontal arrows indicate the position and direction of primers for PCR (Table 1). (E) RT-PCR analysis of the translocated *OCT4/3* gene and the untranslocated *OCT4/3* gene in GBS6 cell, NCR-G2, NCR-G3, NCR-G4, and 3F0664 cells. NCR-G2, NCR-G3, and NCR-G4 cells are embryonal carcinoma cells, and 3F0664 cells are mesenchymal cells. (F) Western blot analysis of EWS-OCT4/3 in GBS6 cells. Western blot analysis was performed using anti-Oct4/3 antibody. EWS-OCT4/3 chimeric protein (~58 kDa) was detected in GBS6 cells. The positions of prestained molecular markers (BIO-RAD) are indicated to the left (kDa).

HLA-ABC (IM1838, Beckman), HLA-DR, DP, DQ (6604366, Beckman), SSEA-1 (MAB4301, Chemicon), SSEA-3 (MAB4303, Chemicon), SSEA-4 (MAB4304, Chemicon), STRO-1 (MAB1038, R and D Systems), TRA-1-60 (MAB4360, Chemicon), and TRA-1-81 (MAB4381, Chemicon) were adopted as primary antibodies. PE-conjugated anti-mouse Ig antibody (550589, Pharmingen), PE-conjugated anti-mouse IgM antibody (555584, Pharmingen) and PE-conjugated anti-rat Ig antibody (550767, Pharmingen) were used as secondary antibodies. X-Mean, the sum of the intensity divided by total cell number, was automatically calculated, and it was adopted for the evaluation of this experiment.

Implantation of cells into mice

GBS6 cells ($>1\times10^7$) were subcutaneously inoculated into an immunodeficient, NOD/Shi-*scid*, IL-2Rγ^{null} mouse (NOG mouse) (CREA, Tokyo, Japan). Subcutaneous specimens were resected at 2 weeks after implantation. The operation protocols were accepted by the Laboratory Animal Care and the Use Committee of the National Research Institute for Child and Health Development, Tokyo (approval number: 2003-002 and 2005-003).

Immunohistochemistry analysis

Immunohistochemical analysis was performed as previously described [34–36] with antibodies to MIC2 (clone# 12E7, cat# M3601, DAKO, Carpinteria, CA, USA), vimentin (clone# V9, cat# M0725, DAKO, Carpinteria, CA, USA), neurofilament protein 70 kDa (NF-L, clone# 2F11, cat# M0762, DAKO, Carpinteria, CA, USA), desmin (clone# D9, cat# 010031, Bio-Science Products AG, Emmenbruecke, Switzerland), smooth muscle actin (clone# 1A4, cat# M0851, DAKO, Carpinteria, CA, USA), and OCT4/3 (clone# C-10, cat# sc-5279, Santa Cruz Biotechnology, Inc., CA, USA) in PBS containing 1% bovine serum albumin. As a methodological control, the primary antibody was omitted. Immunohistochemical analysis of iPS cells was performed according to the manufacturer's protocol [SCR002,

A

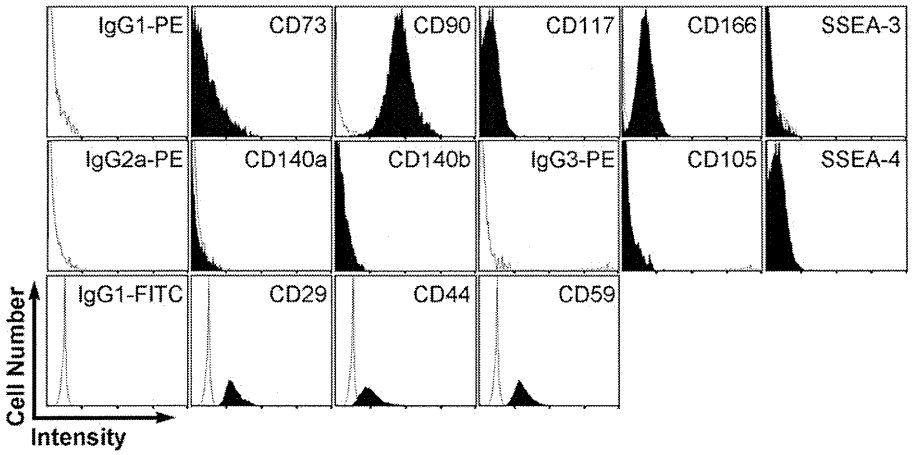

B

Negative (y≦0.1)			Low (0.1<y<1)	Positive (1<y)
CD13	CD106	ABCG2	CD73	CD9
CD14	CD117	HLA-DR,DQ,DP	CD166	CD29
CD24	CD130	SSEA-1		CD44
CD31	CD133	SSEA-3		CD59
CD34	CD135	SSEA-4		CD81
CD45	CD140a	Stro-1		CD90
CD50	CD140b	TRA-1-60		HLA-A,B,C
CD55	CD157	TRA-1-81		
CD105	CD243			

Fig. 2 – Cell surface marker analysis of GBS6 cells. (A) Flow cytometric analysis of cell surface markers in GBS6 cells. The results of CD73, CD90, CD117, CD166 and SSEA-3 were compared with the result of their isotype control, PE-conjugated IgG1. The results of CD140a and CD140b were compared with the result of PE-conjugated IgG2a. The results of CD105 and SSEA-4 were compared with the result of PE-conjugated IgG3. The results of CD29, CD44 and CD59 were compared with the result of FITC-conjugated IgG1. *X*-axis and *Y*-axis indicate the intensity and the cell number, respectively. (B) Summary of cell surface markers. "*y*" is "X-means" subtracted by 'a value of isotype control'; "$y<0.1$", "$0.1<y<1$", and "$1<y$" were determined "negative", "low" and "positive", respectively.

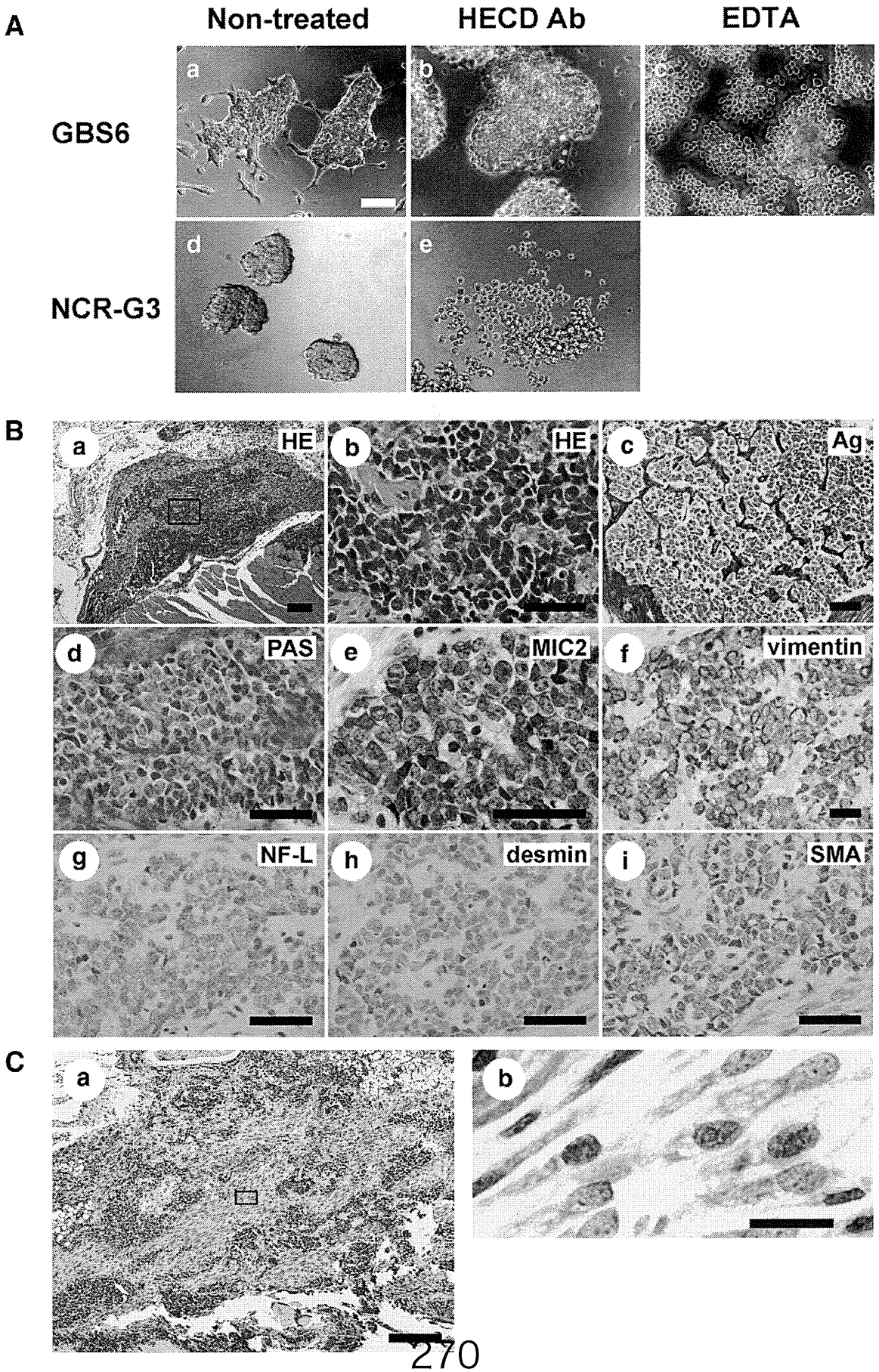
A
Non-treated
HECD Ab
EDTA
GBS6
NCR-G3
a
b
c
d
e
B
HE
HE
Ag
PAS
MIC2
vimentin
NF-L
desmin
SMA
C

Chemicon (Millipore)]. Primary antibodies included Oct-3/4 (C-10) (diluted at 1:300, sc-5279, Santa Cruz), NANOG (diluted at 1:300, RCAB0003P, ReproCELL), SSEA-4 (diluted at 1:300, MAB4304, CHEMICON), and TRA-1-60 (diluted at 1:300, MAB4360, CHEMICON). Secondary antibodies used were Alexa Fluor 546 Goat Anti-mouse IgG, 2 mg/mL (diluted at 1:300, A11003, Invitrogen), Alexa Fluor 488 Goat Anti-rabbit IgG, 2 mg/mL (diluted at 1:300, A11008, Invitrogen), and Alexa Fluor 488 Goat Anti-mouse IgG, 2 mg/mL, F (ab′)2 fragment (diluted at 1:300, A11017, Invitrogen). Nuclei were stained with 1 μg/mL DAPI (40043, Biotium).

Quantitative RT-PCR

RNA was extracted from cells using the RNeasy Plus Mini kit (Qiagen). An aliquot of total RNA was reverse transcribed by using an oligo (dT) primer. For the thermal cycle reactions, the cDNA template was amplified (ABI PRISM 7900HT Sequence Detection System) using the Platinum Quantitative PCR SuperMix-UDG with ROX (11743-100, Invitrogen) under the following reaction conditions: 40 cycles of PCR (95 °C for 15 s and 60 °C for 1 min) after an initial denaturation (95 °C for 2 min). Fluorescence was monitored during every PCR cycle at the annealing step. The authenticity and size of the PCR products were confirmed using a melting curve analysis (using software provided by Applied Biosystems) and a gel analysis. mRNA levels were normalized using *GAPDH* as a housekeeping gene. POU5F1-2-F and POU5F1-3-R primers were used to detect the *OCT4/3* gene (see Table 1, D and F).

Chromatin immunoprecipitation (ChIP) assays

Chromatin immunoprecipitation was performed according to the instructions of the EZ ChIP Chromatin Immunoprecipitation Kit (17-371, Upstate Biotechnology Inc., Chicago, IL, USA). Histone and DNA were cross-linked with 1% formaldehyde for 10 min at room temperature and formaldehyde was then inactivated by the addition of 125 mM glycine. The chromatin was then sonicated to an average DNA fragment length of 200 to 1000 bp. Soluble chromatin reacted with and without anti-acetylated Histone H3 (06-599, Upstate Biotechnology Inc., Chicago, IL, USA), and anti-acetylated Histone H4 (06-866, Upstate Biotechnology Inc., Chicago, IL, USA). The immunocomplex was purified and collected in elution buffer (0.1 M $NaHCO_3$, 1% sodium dodecyl sulfate). Crosslinking was then reversed using elution buffer containing RNase A (0.03 mg/mL) and NaCl (0.3 M) by incubation for 4 h at 65 °C. Supernatant obtained without antibody was used as the input control. The DNA was treated with proteinase K for 1 h at 45 °C and purified. For all ChIP experiments, quantitative PCR analyses were performed in real time as described in this manuscript. Relative occupancy values were calculated by determining the apparent immunoprecipitation efficiency (ratios of the amount of immunoprecipitated DNA to that of the input sample) and normalized to the level observed at a control region. For all the primers used, each gave a single product of the right size adult stem cell confirmed by agarose gel electrophoresis and dissociation curve analysis. These primers also gave no DNA product in the no-template control. The following three primer sets for human *OCT4/3*, as previously described [26], were adopted for real-time PCR to quantitate the ChIP-enriched DNA: human *POU5F1*-A (-2613/-2396), 5′-GGG GAACCTGGAGGATGG-CAAGCTGAGAAA-3′ and 5′-GGCCTGGTGGGGGTGGGAGG AACAT-3′; human *POU5F1*-B (-1779/-1563), 5-CCTGCACCCCTCCACAAATCACTC GC-3′ and 5′-TGCAATCCCCTCAAAGACTGAGCCTCAGAC-3′ ; human *POU5F1*-C (-237/-136), 5′-GAGGGGCGCCAGTTGTGTCTCCCGGTTTT-3′ and 5′-GGGAGGTGGG GGGAGAAACTGAGGCGAAGG-3′.

DNA methylation analysis

The NCR-G2 (JCRB cell bank number; JCRB1167) [32], NCR-G3 (JCRB cell bank number; JCRB1168) [32], GBS6, and Yub636BM (human bone marrow cells derived from an extra digit) cells were prepared for this assay. Genomic DNA was isolated using DNeasy Blood and Tissue Kit (69504, QIAGEN). Primers were selected from the CpG island regions with homogenous CpG site methylation patterns. The target region of the genes used for methylation analysis and the primer sequences used for PCR amplification are shown in Table 4. One of the two primers in the PCR amplification of the target regions is tagged with a T7 promoter sequence: cagtaatacgactcactatagggagaaggct. The PCR reactions were carried out in a total volume of 5 μL using 1 pmol of each primer, 40 μM dNTP, 0.1 U HotStar Taq DNA polymerase (QIAGEN), 1.5 mM $MgCl_2$, 5× PCR buffer (final concentration 1×), and bisulfite-converted DNA. The reaction mix was preactivated for 15 min at 95 °C. The reactions were amplified in 45 cycles of 95 °C for 20 s, 62 °C for 30 s, and 72 °C for 30 s followed by 72 °C for 3 min. Unincorporated dNTPs were dephosphorylated by adding 1.7 μL DNase-free water and 0.3 U Shrimp Alkaline Phosphatase (SAP). The reaction was incubated at 37 °C for 20 min and SAP was then heat-inactivated for 10 min at 85 °C. Typically, 2 μL of the PCR reaction was directly used as a template in a 6.5 μL combined transcription-cleavage reaction. Twenty units of T7 polymerase (Epicentre) were used to incorporate either dCTP or dTTP in the transcripts. Ribonucleotides at 1 mM and the dNTP substrate at 2.5 mM were used. RNase A (Sequenom) was included to cleave the in vitro transcript. The mixture was then further diluted with water to a final volume of 27 μL. Conditioning of the phosphate backbone prior to MALDI-TOF MS was achieved by the addition of 6 mg CLEAN resin (Sequenom). The cleavage reaction samples (15 nL) were dispensed onto silicon

Fig. 3 – In vitro and in vivo characteristics of GBS6 cells. (A) Ca++-dependent, E-cadherin-independent adhesion of GBS6 cell aggregates. GBS6 cells (a) were unaffected by the antibody to E-cadherin (b), but were dissociated by EDTA, Ca++ chelator (c). In contrast, NCR-G3 cells (d), serving as a control since they are E-cadherin-dependent, were dissociated and induced to death by the antibody to E-cadherin (e). Scale bar: 100 μm. (B) Immunohistochemical analysis of GBS6 cells implanted into the subcutaneous tissue of NOG mice. GBS6 cells at 2 weeks after implantation (a, b: hematoxylin and eosin stain, c: silver stain, d: PAS stain) were examined for immunohistochemical analysis using antibodies to MIC2 (e), vimentin (f), neurofilament protein 70 kDa (g: NF-L), desmin (h), and smooth muscle actin (i: SMA). Scale bars: 200 μm (a) and 50 μm (b–i). (C) Immunohistochemical analysis with the anti-OCT4/3 antibody of GBS6 cells implanted into the subcutaneous tissue of NOG mice. GBS6 cells at 2 weeks after implantation were examined for immunohistochemical analysis using antibodies to OCT4/3. The higher-magnification image of the region enclosed by a square in "a" (b). Scale bars: 200 μm (a) and 20 μm (b).

chips preloaded with matrix (SpectroCHIP, Sequenom). Mass spectra were collected using a MassARRAY mass spectrometer (Sequenom). Spectra were analyzed using proprietary peak picking and spectra interpretation tools (EpiTYPER, Sequenom).

For analysis of DNA methylation, we examined the methylation-dependent C/T sequence changes introduced by bisulfite treatment. Those C/T changes are reflected as G/A changes on the reverse strand and hence result in a mass difference of 16 kDa for

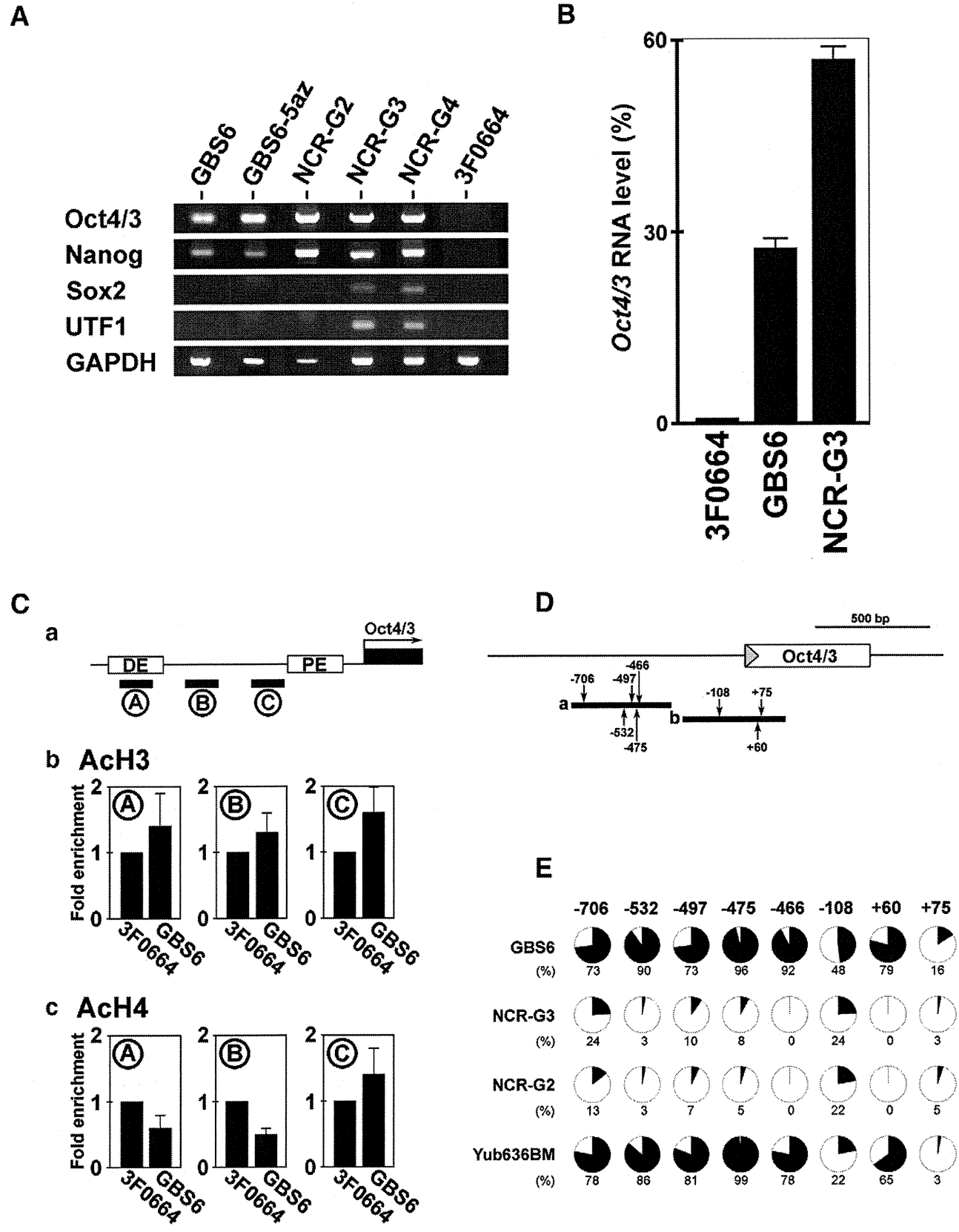

each CpG site enclosed in the cleavage products generated from the RNA transcript. The mass signals representing nonmethylated DNA and those representing methylated DNA, built signal pairs, which are representative for the CpG sites within the analyzed sequence substring. The intensities of the peaks were compared, and the relative amount of methylated DNA was calculated from this ratio. The method yields quantitative results for each of these sequence-defined analytic units referred to as CpG units, which contain either one individual CpG site or an aggregate of subsequent CpG sites.

Plasmid construction

Each open reading frame of human *OCT4/3* and *SOX2* was amplified by RT-PCR using the RNA extracted from NCR-G2 cells (JCRB cell bank number; JCRB1167) [32], a complex-type germ cell tumor cell line. Also, those of *c-MYC* and *KLF4* were amplified by RT-PCR using the RNA extracted from the bone marrow stromal cell line, UET13. A Gateway cassette composed of an attR1/R2 flanked CmR and ccdB (Invitrogen) was amplified by PCR and ligated into the Eco RI/Not I site of pMXs retroviral expression vector to create pMXs-DEST [37]. PCR amplification was performed by using KOD-Plus-DNA polymerase (KOD-201, TOYOBO). The constructs were confirmed by sequencing.

Retroviral infection and iPS cell generation

293FT cells (Invitrogen) were plated at 2×10^6 cells per 100 mm dish and incubated overnight. The next day, the cells were co-transfected with pMXs-OCT4/3, pMXs-SOX2, pMXs-c-MYC, pMXs-KLF4, pCL-GagPol, and pHCMV-VSV-G vectors with TransIT-293 reagent (Mirus, Madison, WI). Twenty-four hours after transfection, the medium was replaced with a new medium, which was collected after 48 h as the virus-containing supernatant. MRC-5 cells were seeded at 1×10^5 cells per 35 mm dish 1 day before infection. The virus-containing supernatants were filtered through a 0.45 μm pore-size filter, ultracentrifuged at 8500 rpm for 16 h, and then resuspended in DMEM (D6429, SIGMA) supplemented with 4 mg/mL polybrene (Nacalai Tesque). Equal amounts of concentrated supernatants containing each of the four retroviruses were mixed, transferred to MRC-5 cells, and incubated for 8 h. The MRC-5 cells were cultured for 4 days and replated on an irradiated MEF feeder layer in 100 mm dish. The medium was replaced with the iPSellon medium supplemented with 10 ng/mL bFGF. One-half of the medium was changed every day and the cells were cultured up to 30 days after a day of infection. Colonies were picked up and transferred into 0.2 mL of iPSellon medium when colonies appeared. The colonies were mechanically dissociated to small clumps by pipeting up and down or mechanically cut using a STEMPRO EZPassage disposable passaging tool (23181010, Invitrogen). The cell suspension was transferred on irradiated MEF feeder in 4-well plates [176740, Nunc (Thermo Fisher Scientific)]. We define this stage as passage 1.

Teratoma formation

iPS cells were harvested by accutase treatment, collected into tubes, and centrifuged, and the pellets were suspended in the iPSellon medium. The same volume of Basement Membrane Matrix (354234, BD Biosciences) was added to the cell suspension. Cells (1×10^7) were implanted subcutaneously to a BALB/c-*nu/nu* mouse (CREA, Japan) for 4 weeks. Tumors were dissected and fixed with PBS containing 4% paraformaldehyde. Paraffin-embedded tissue was sliced and stained with hematoxylin and eosin.

GeneChip expression analysis

Total RNA was extracted from cells using the RNeasy Mini Kit (74104, Qiagen, Valencia, CA). Genomic DNA was eliminated by DNase I (2215A, TAKARA BIO INC.) treatments. From all RNA samples, 5 μg of total RNA was used as a starting material for the microarray sample preparation. Double-stranded cDNA was synthesized from DNase-treated total RNA, and the cDNA was subjected to in vitro transcription in the presence of biotinylated nucleoside triphosphates using the Enzo BioArray HighYield RNA Transcript Labeling Kit (Enzo Life Sciences, Inc., Farmingdale, NY), according to the manufacturer's protocol (One-Cycle Target Labeling and Control Reagent package). Human-genome-wide gene expression was examined with the Human Genome U133A Probe array (GeneChip, Affymetrix), which contains the oligonucleotide probe set for approximately 23,000 full-length genes and expressed sequence tags (ESTs), according to the manufacturer's protocol (Expression Analysis Technical Manual and GeneChip small sample target labeling Assay Version 2 technical note, http://www.affymetrix.com/support/technical/index.affx) as previously described [5]. Hierarchical clustering and principle component

Fig. 4 – Expression of the *OCT4/3* gene and histone modification of the *OCT4/3* promoter in GBS6 cells. (A) Expression of embryonic stem cell-enriched genes in GBS6, NCR-G2, NCR-G3, NCR-G4, and 3F0664 cells. GBS6 cells expressed the *OCT4/3* and *NANOG* genes, but not the *SOX2* and *UTF1* genes. NCR-G2 cells expressed the *OCT4/3* and *NANOG* genes; both NCR-G3 cells and NCR-G4 cells expressed the *OCT4/3*, *NANOG*, *SOX2* and *UTF1* genes. 3F0664 mesenchymal cells did not express these four kinds of embryonic stem cell-enriched genes. POU5F1-1a-F and POU5F1-1a-R (Table 1) were used to amplify the endogenous *OCT4/3* gene. (B) Quantitative PCR analysis to assess the expression level of *OCT4/3* mRNA in GBS6. *OCT4/3* mRNA level is expressed relative to 3F0664 cells control. (C) Real-time PCR to quantitate the ChIP-enriched DNA using acetylated Histone H3 and acetylated Histone H4 antibodies. Schematic of the location of the amplicons (A–C) used to detect ChIP-enriched fragments in *OCT4/3* shown relative to the distal enhancer (DE)/CR4 region, to the proximal enhancer (PE), and to transcription start site (arrow) (a). The relative levels of acetylated Histone H3 (b) and acetylated Histone H4 (c) modifications were detected in GBS6 cells and 3F0664 cell control. GBS6 cells are represented by black bars and 3F0664 cells by open bars. (D) DNA methylation analysis in the promoter region of the *OCT4/3* gene. The target regions of *OCT4/3* used for the quantitative DNA methylation analysis. Region 'a' and Region 'b' include 5 (−706, −532, −497, −475, −466) and 3 (−108, +60, +75) CpG sites, respectively. The positions of CpG sites are relative to the *OCT4/3* transcription start site (gray triangle). (E) The relative amount of methylated DNA ratio (%) at each CpG site is indicated as the black area in the pie chart.

analysis were performed to group mesenchymal cells obtained from bone marrow into subcategories (http://lgsun.grc.nia.nih.gov/ANOVA/).

Results

Establishment of human cells of mesenchymal origin with overexpression of the translocated POU5F1/OCT4/3 gene

To investigate whether cells of mesenchymal origin acquire an embryonic phenotype, a novel human cell line termed GBS6 was established from the pelvic bone tumor, of which histology shows diffuse proliferation of undifferentiated tumor cells with oval nuclei and scant but short spindle cytoplasm [31]. The generated cells grew attached to the dish as a polygonal cell sheet with cell aggregates forming in the center (Figs. 1A, B), and retained the reciprocal translocation, t(6; 22), detected in the original tumor (Fig. 1C). The *EWS-OCT4/3* chimeric gene expression also remained (Figs. 1D, E and Table 1). Embryonal carcinoma (EC) cells, i.e., NCR-G2, NCR-G3, and NCR-G4, served as control cells expressing the endogenous *OCT4/3* gene. Immunoblot analysis revealed that EWS-OCT4/3 fusion protein was expressed in GBS6 cells (Fig. 1F).

Cell surface markers of GBS6 cells

GBS6 cell surface markers were evaluated by flow cytometric analysis (Fig. 2). The results showed that GBS6 cells were strongly positive (Positive; Fig. 2B) for CD9, CD29 (integrin β1), CD44, CD59, CD81, CD90 (Thy-1) and HLA-A,B,C (HLA class I); weakly positive (Low; Fig. 2B) for CD73 and CD166 (ALCAM); negative (Negative; Fig. 2B) for CD55, CD105 (endogrin), CD140a (PDGFRα), and CD140b (PDGFRβ). The lack of CD13, CD55, CD105, CD106, CD140a, and CD140b in GBS6 cells suggests that the surface markers of GBS6 cells are different from those of conventional mesenchymal cells [10,38,39].

E-cadherin-independent growth of GBS6 cells

To investigate whether GBS6 cells survive dependent on E-cadherin-like human embryonic cells, the cells were treated by an inhibitory antibody to E-cadherin (HECD Ab) and EDTA (Fig. 3A). GBS6 cell survival was unaffected by the E-cadherin antibody but affected by EDTA (Fig. 3A-a, b, c). In contrast, NCR-G3 cells, human embryonal carcinoma cells that proliferate in an E-cadherin-dependent manner, were dissociated and induced to apoptosis by the E-cadherin antibody (Fig. 3A-d, e).

Implantation of GBS6 cells into immunodeficient mice

To investigate an in vivo phenotype of GBS6 cells, the cells were intramuscularly injected into immunodeficient NOG mice and examined by histopathology and immunohistochemistry (Fig. 3B). The injected cells exhibited an undifferentiated phenotype with oval nuclei and scant spindle cytoplasm (Fig. 3B-b), and showed an alveolar configuration (Fig. 3B-c). The cells were negative by the PAS stain (Fig. 3B-d). The cells were immunohistochemically positive for MIC2 and vimentin (Fig. 3B-e, f), and negative for neurofilament, desmin, and smooth muscle actin (Fig. 3B-g, h, i). The cells retained OCT4/3 in their nuclei even after implantation (Fig. 3C).

Expression of ES-enriched genes

To determine if GBS6 cells express ES cell-enriched genes, that is, the *OCT4/3*, *NANOG*, *SOX2*, and *UTF1* genes, RT-PCR with specific primer sets (Table 2) and gene chip analyses were performed. GBS6 cells expressed the endogenous *OCT4/3* and *NANOG* genes like NCR-G2, NCR-G3, and NCR-G4 embryonal carcinoma cells, but did not express the *SOX2* and *UTF1* genes (Fig. 4A). The results of the RT-PCR analysis were compatible with those of the gene chip analysis (GSE8113, Table 3). To compare the expression level of stem cell-specific genes in GBS6 cells, ES cells, and mesenchymal cells, we performed a quantitative RT-PCR analysis. The expression level of *OCT4/3* was about half that of human EC cells, but was more than twenty-five times that of 3F0664 mesenchymal cells (Fig. 4B). The results show that the expression level of *OCT4/3* is comparable to that of human EC cell.

To determine if the cis-regulatory element of the *OCT4/3* gene has so-called open chromatin structure, we performed the chip analysis using antibodies to acetylated H3 and acetylated H4 (Fig. 4C). The results show that acetylated histone levels which the *OCT4/3* promoter is wrapped around in GBS6 cells are comparable with those in 3F0664 mesenchymal cells. We also performed methylation analysis of the *OCT4/3* gene in GBS6 cells because the expression of *OCT4/3* gene is regulated by methylation (Figs. 4D, E and Table 4). The promoter region of the *OCT4/3* gene was heavily methylated in GBS6 cells as compared with human NCR-G3 embryonal carcinoma cells expressing the *OCT4/3* gene at a high level.

Cell reprogramming assay

To investigate if chimeric EWS-OCT4/3 induces iPS cells like native OCT4/3, we performed Yamanaka's reprogramming assay on MRC-5 human fetal lung fibroblasts (Fig. 5A), using the chimeric *EWS-OCT4/3* construct with the *KLF-4*, *SOX2*, and *c-MYC* genes according to the conventional protocol [40] with some modifications. We failed to obtain iPS cells using the *EWS-OCT4/3*, *KLF-4*, *SOX2*, and *c-MYC* constructs (Fig. 5B), albeit trials of three independent experiments, whereas, for a control, we successfully generated 101 clones of iPS cells from MRC-5 cells using the *OCT4/3*, *KLF-4*, *SOX2*, and *c-MYC* constructs (Fig. 5C). The iPS cells generated from MRC-5 cells expressed human ES cell-specific surface antigens (Figs. 5D–G). In vivo implantation analysis showed that iPS cells generated various tissues including neural tissues (Fig. 5H: ectoderm), cartilage (Fig. 5I: mesoderm),

Table 4 – Primers used for PCR amplification of the bisulfite-converted DNA.

Name	Sequence	Size (bp)
Region 'a'	Forward: 5′ TTG GTT ATT GTG TTT ATG GTT GTT G 3′ Reverse: 5′ TAA ACC AAA ACA ATC CTT CTA CTC C 3′	437
Region 'b'	Forward: 5′ TTT GGG TAA TAA AGT GAG ATT TTG TTT 3′ Reverse: 5′ CTA ACC CTC CAA AAA AAC CTT AAA A 3′	452

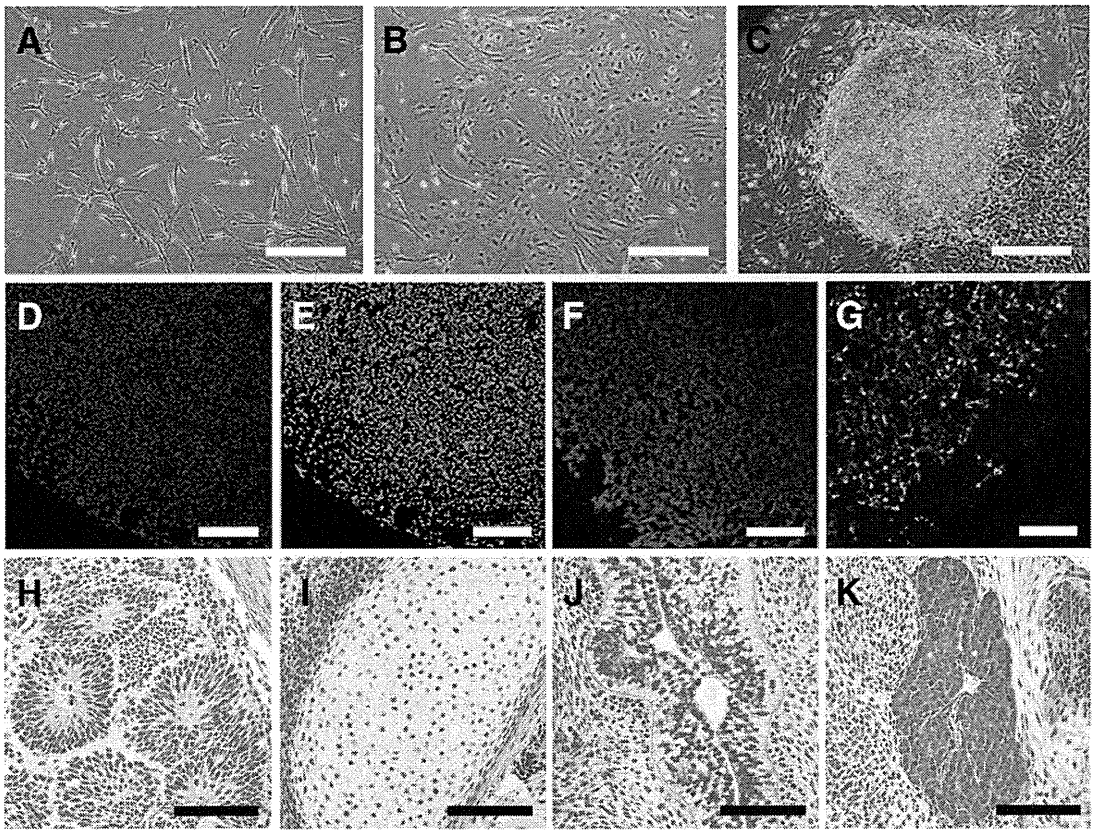

Fig. 5 – Induction of iPS cells from MRC-5 cells and teratoma formation. (A) Morphology of MRC-5 cells. (B) Morphology of cells using *EWS-OCT4/3*, *KLF-4*, *SOX2*, and *c-MYC* genes at Day 30 after infection. (C) Morphology of established iPS cell (clone 16: Fetch) colony using *OCT4/3*, *KLF-4*, *SOX2*, and *c-MYC* genes at Day 20 after infection. (D–G) Immunocytochemistry for OCT4/3 (D), NANOG (E), SSEA-4 (F), and TRA-1-60 (G). Nuclei were stained with DAPI. Bars = 500 μm (A–C), and 200 μm (D–G). In addition, chromosomal G-band analyses showed that human iPS cells from MRC-5 had a normal karyotype of 46XY (not shown). The analysis of short tandem repeat shows that novel iPS cells from MRC-5 cells were not a result of cross-contamination. Hematoxylin and eosin staining of teratoma derived from the generated iPS cells. Cells (1×10^7) were implanted subcutaneously to a BALB/c-*nu*/*nu* mouse for 4 weeks. Histological examination showed that the tumor contained various tissues, neural tissues (H; ectoderm), cartilage (I; mesoderm), a gut-like epithelial tissue (J; endoderm), and a hepatic tissue (K; endoderm). Bars = 100 μm (H–K).

a gut-like epithelial tissue (Fig. 5J: endoderm), and a hepatic tissue (Fig. 5K: endoderm). These results imply that the chimeric *EWS-OCT4/3* gene does not participate in reprogramming of somatic cells.

Principle component analysis of global gene expression in GBS6 cells

To determine whether GBS6 cells are categorized into embryonal cells or mesenchymal cells, global gene expression patterns of GBS6 cells, embryonal carcinoma cells (NCR-G2, NCR-G3, and NCR-G4), yolk sac tumor cells (NCR-G1), and marrow stromal cells (3F0664, H4-1, and Yub10F) were further analyzed by principle component analysis (PCA), which reduces high-dimensionality data into a limited number of principle components (Fig. 6). The first principle component (PC1) captures the largest contributing factor of variation, which characterizes the differential expression of genes. As we were interested in the differential gene expression component, we plotted the position of each cell type against the PC1, PC2, and PC3 axis in three-dimensional space by using virtual reality modeling language (Fig. 6A). Close examination of the 3D model identified PC1 as the most representative view of the 3D model. PC1 axis direction is therefore used to characterize the differential gene expression (Fig. 6B). In addition, hierarchical analysis of the cells analyzed for global gene expression revealed that GBS6 cells are categorized into embryonal carcinoma cells and yolk sac tumor cells, i.e., NCR-G1, -G2, -G3, and -G4 cells (Fig. 6C).

Discussion

In this study, we generated a cell line with a transitional form between mesenchymal cells and embryonic stem cells. Loss of mesenchyme-specific cell markers, i.e., CD13, CD55, CD105, CD106, CD140a and CD140b, and modification of cell survival with the calcium chelator indicate that GBS6 cells are no longer mesenchymal cells. Global and drastic differences in gene expression with the GeneChip analysis support the conclusion that GBS6 cells no longer exhibit the profile of mesenchymal cells. It is also noteworthy that this transition phenotype is reliably inherited ex vivo after a series of in vitro passages.

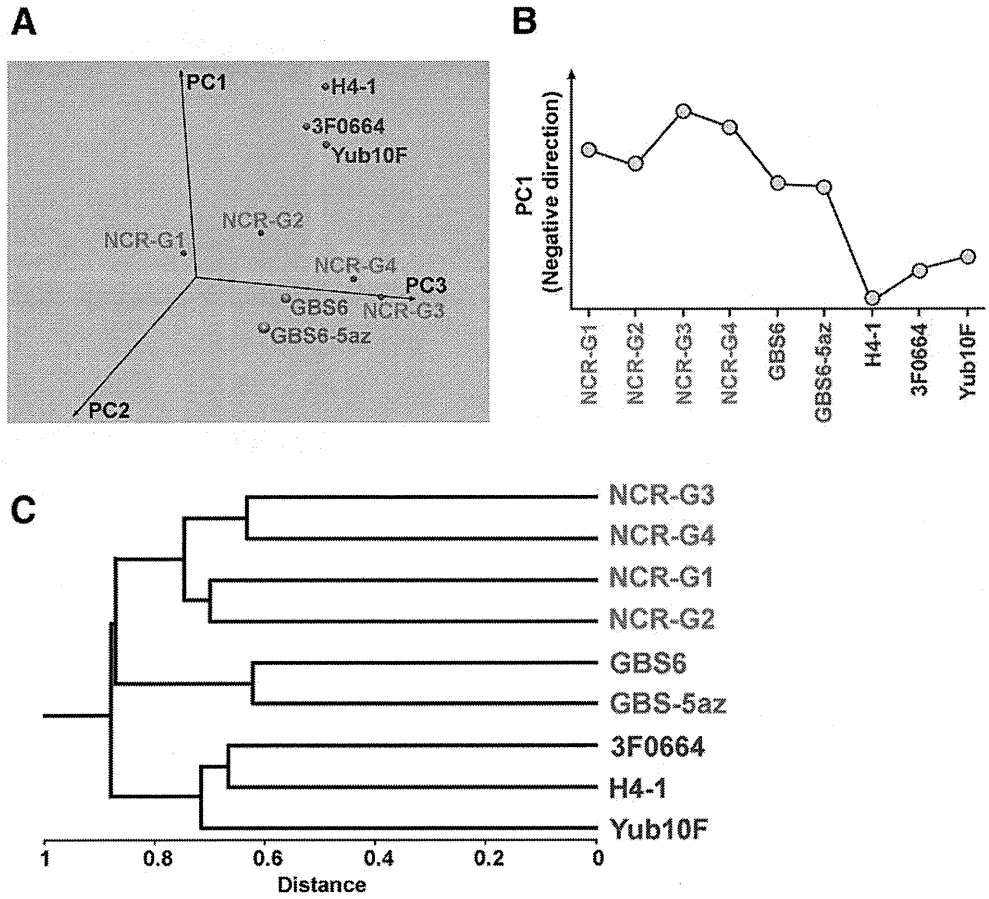

Fig. 6 – Principal component analysis and hierarchical clustering of gene expression in GBS6 cells, embryonal carcinoma cells, and bone marrow cells. (A) 3D-representation of principle component analysis. (B) Principal components of PC1 axis, negative direction. (C) Hierarchical clustering analysis of averages.

OCT4/3 function and its physiological partner EWS in embryonic transition

ES-like cells or iPS cells are generated from murine fibroblasts by transfecting four genes, i.e., *OCT4/3*, *SOX2*, *KLF-4* and *c-MYC* are necessary for the mesenchymal–embryonic transition [1–3]. However, OCT4/3 alone is not sufficient to confer embryonic phenotypes to human bone marrow-derived cells, NIH3T3 cells (data not shown) or embryonic fibroblasts [1]. EWS and OCT4/3 are directly bound both in vitro and in vivo [41]; in other words, EWS is a binding partner of OCT4/3. Therefore, the EWS-OCT4/3 protein in GBS6 cells is considered a fusion between physiological partners. EWS and OCT4/3 are co-expressed in the pluripotent mouse and human ES cells. To investigate if the EWS-OCT4/3 has a transcriptional activity, we performed the luciferase assay. The results show that the chimeric *EWS-OCT4/3* gene has comparable or higher transcriptional activity than the native *OCT4/3* gene does (Supplementary Fig. S1). Ectopic expression of non-chimeric EWS enhances the transactivation activity of OCT4/3; the N-terminal QSY domain of EWS and the C-terminal POU domain function as a transcriptional activation and DNA binding, respectively [42,43]. The *OCT4/3* gene is overexpressed under the cis-regulatory element of the *EWS* gene [31], and the functional co-operation of OCT4/3 and EWS at a protein level to transcriptional activation may lead to embryonic transformation in GBS6 cells. Converting mesenchymal cells to embryonic cells opposes the usual direction of ES cell differentiation [44]; and this is achieved by chimeric OCT4/3 with physiological co-activator EWS driven by the potent cis-regulatory element of the *EWS* gene [31]. This phenotypic conversion requires the molecular reprogramming of mesenchymal cells with new instructions.

Mesenchymal to embryonic "incomplete" transition by overexpression of chimeric OCT4/3

OCT4/3 fused to *EWS* not only participates in oncogenesis [29,31], but also contributes to mesenchymal–embryonic transition, at least in part from the viewpoint of global gene expression profiles and cell surface markers (Figs. 2 and 6). GBS6 cells are subcategorized into groups of cells derived from testicular germ cell tumors (Fig. 6A, cells with embryonic phenotypes are shown in pink), and the PC1 axis indicates transition from mesenchymal cell group to embryonal cell group (Fig. 6B). This transition was, however, incomplete; some of the ES-specific genes were not reactivated. OCT4/3 is a member of the POU family of transcription factors, is expressed in pluripotent ES cells, including primordial germ cells [17–21], and functions as a master switch in differentiation by regulating cells that have, or can develop, pluripotent

276

potential. However, tight chromatin structure in GBS6 cells may render OCT4/3 recognition sequences inaccessible [45]. The OCT4/3 recognition sequences have been found in the cis-regulatory elements of the FGF-4 and CD140a/platelet-derived growth factor receptor-α gene [46], but GBS6 cells are indeed negative for CD140a (Fig. 2B). Alternatively, the lack of other essential transcription factors such as SOX2 and UTF1 (Fig. 4A, Table 3) and/or co-factors may be a cause of "incomplete" transition. Interestingly, this transition phenotype is reliably inherited ex vivo after a series of in vitro passages, and this may also be attributed to the function of OCT4/3 that is critical for self-renewal of embryonic stem cells [24].

Mesenchymal to epithelial transition is observed in physiological and pathological conditions [47–50]. In contrast, mesenchymal–embryonic transition has been achieved in an artificial experimental condition in vitro [1–3]. Homogenous positive staining for OCT4/3 in embryonal carcinoma cells supports the model that the encoded protein is crucial, and the absence of OCT4/3 in non-embryonal carcinoma cells is in agreement with the inability to generate pluripotent stem cells [51]. The cell line generated in this study with overexpression of chimeric OCT4/3, although this is just one case of rare human immortalized cells, provides us with insight into cell plasticity involving OCT4/3 that is essential for ES cell maintenance and into the complexity required for changing cellular identity.

Acknowledgments

We would like to express our sincere thanks to Michiyo Nasu for histological analysis, Yoriko Takahashi for data mining, and Kayoko Saito for secretary work. This study was supported by grants from the Ministry of Education, Culture, Sports, Science and Technology (MEXT) of Japan and Health and Labor Sciences Research Grants; by Research on Health Science Focusing on Drug Innovation from the Japan Health Science Foundation; by the Program for Promotion of Fundamental Studies in Health Science of the Pharmaceuticals and Medical Devices Agency; by the grant from Terumo Life Science Foundation; by a research Grant for Cardiovascular Disease from the Ministry of Health, Labor and Welfare; and by a Grant for Child Health and Development from the Ministry of Health, Labor and Welfare.

Appendix A. Supplementary data

Supplementary data associated with this article can be found, in the online version, at doi:10.1016/j.yexcr.2009.06.016.

REFERENCES

[1] K. Takahashi, S. Yamanaka, Induction of pluripotent stem cells from mouse embryonic and adult fibroblast cultures by defined factors, Cell 126 (2006) 663–676.
[2] K. Okita, T. Ichisaka, S. Yamanaka, Generation of germline-competent induced pluripotent stem cells, Nature 448 (2007) 313–317.
[3] M. Wernig, A. Meissner, R. Foreman, T. Brambrink, M. Ku, K. Hochedlinger, B.E. Bernstein, R. Jaenisch, In vitro reprogramming of fibroblasts into a pluripotent ES-cell-like state, Nature 448 (2007) 318–324.
[4] M.J. Go, C. Takenaka, H. Ohgushi, Forced expression of Sox2 or Nanog in human bone marrow derived mesenchymal stem cells maintains their expansion and differentiation capabilities, Exp. Cell Res. 314 (2008) 1147–1154.
[5] T. Mori, T. Kiyono, H. Imabayashi, Y. Takeda, K. Tsuchiya, S. Miyoshi, H. Makino, K. Matsumoto, H. Saito, S. Ogawa, M. Sakamoto, J. Hata, A. Umezawa, Combination of hTERT and bmi-1, E6, or E7 induces prolongation of the life span of bone marrow stromal cells from an elderly donor without affecting their neurogenic potential, Mol. Cell. Biol. 25 (2005) 5183–5195.
[6] R.H. Lee, B. Kim, I. Choi, H. Kim, H.S. Choi, K. Suh, Y.C. Bae, J.S. Jung, Characterization and expression analysis of mesenchymal stem cells from human bone marrow and adipose tissue, Cell. Physiol. Biochem. 14 (2004) 311–324.
[7] J.G. Toma, M. Akhavan, K.J. Fernandes, F. Barnabe-Heider, A. Sadikot, D.R. Kaplan, F.D. Miller, Isolation of multipotent adult stem cells from the dermis of mammalian skin, Nat. Cell Biol. 3 (2001) 778–784.
[8] C.H. Cui, T. Uyama, K. Miyado, M. Terai, S. Kyo, T. Kiyono, A. Umezawa, Menstrual blood-derived cells confer human dystrophin expression in the murine model of duchenne muscular dystrophy via cell fusion and myogenic transdifferentiation, Mol. Biol. Cell 18 (2007) 1586–1594.
[9] O.K. Lee, T.K. Kuo, W.M. Chen, K.D. Lee, S.L. Hsieh, T.H. Chen, Isolation of multipotent mesenchymal stem cells from umbilical cord blood, Blood 103 (2004) 1669–1675.
[10] M. Terai, T. Uyama, T. Sugiki, X.K. Li, A. Umezawa, T. Kiyono, Immortalization of human fetal cells: the life span of umbilical cord blood-derived cells can be prolonged without manipulating p16INK4a/RB braking pathway, Mol. Biol. Cell 16 (2005) 1491–1499.
[11] X. Zhang, A. Mitsuru, K. Igura, K. Takahashi, S. Ichinose, S. Yamaguchi, T.A. Takahashi, Mesenchymal progenitor cells derived from chorionic villi of human placenta for cartilage tissue engineering, Biochem. Biophys. Res. Commun. 340 (2006) 944–952.
[12] E.H. Allan, P.W. Ho, A. Umezawa, J. Hata, F. Makishima, M.T. Gillespie, T.J. Martin, Differentiation potential of a mouse bone marrow stromal cell line, J. Cell. Biochem. 90 (2003) 158–169.
[13] H. Imabayashi, T. Mori, S. Gojo, T. Kiyono, T. Sugiyama, R. Irie, T. Isogai, J. Hata, Y. Toyama, A. Umezawa, Redifferentiation of dedifferentiated chondrocytes and chondrogenesis of human bone marrow stromal cells via chondrosphere formation with expression profiling by large-scale cDNA analysis, Exp. Cell Res. 288 (2003) 35–50.
[14] S. Makino, K. Fukuda, S. Miyoshi, F. Konishi, H. Kodama, J. Pan, M. Sano, T. Takahashi, S. Hori, H. Abe, J. Hata, A. Umezawa, S. Ogawa, Cardiomyocytes can be generated from marrow stromal cells in vitro, J. Clin. Invest. 103 (1999) 697–705.
[15] N. Nishiyama, S. Miyoshi, N.M. Hida, T. Uyama, K. Okamoto, Y. Ikegami, K. Miyado, K. Segawa, M. Terai, M. Sakamoto, S. Ogawa, A. Umezawa, The significant cardiomyogenic potential of human umbilical cord blood-derived mesenchymal stem cells in vitro, Stem Cells 25 (2007) 2017–2024.
[16] J. Deng, B.E. Petersen, D.A. Steindler, M.L. Jorgensen, E.D. Laywell, Mesenchymal stem cells spontaneously express neural proteins in culture and are neurogenic after transplantation, Stem Cells 24 (2006) 1054–1064.
[17] H.R. Scholer, G.R. Dressler, R. Balling, H. Rohdewohld, P. Gruss, Oct-4: a germline-specific transcription factor mapping to the mouse t-complex, EMBO J. 9 (1990) 2185–2195.
[18] K. Okamoto, H. Okazawa, A. Okuda, M. Sakai, M. Muramatsu, H. Hamada, A novel octamer binding transcription factor is differentially expressed in mouse embryonic cells, Cell 60 (1990) 461–472.
[19] M.H. Rosner, M.A. Vigano, K. Ozato, P.M. Timmons, F. Poirier, P.W. Rigby, L.M. Staudt, A POU-domain transcription factor in early

277